

**AAPG HEDBERG CONFERENCE**  
**“NATURAL GAS GEOCHEMISTRY: RECENT DEVELOPMENTS, APPLICATIONS, AND TECHNOLOGIES”**  
**MAY 9-12, 2011 – BEIJING, CHINA**

**Geochemical Controls on Shale Microstructural Evolution**

Nicholas Drenzek<sup>1</sup>, John Valenza<sup>1</sup>, Hendrik Grotheer<sup>1</sup>, Flora Marques<sup>1</sup>, Michael Herron<sup>1</sup>,  
Sean Sylva<sup>2</sup>, Jeff Seewald<sup>2</sup>

<sup>1</sup>Schlumberger-Doll Research, Cambridge, MA 02139 USA  
<sup>2</sup>Woods Hole Oceanographic Institution, Woods Hole, MA 02543 USA

The complex chemical and structural properties of shale source rocks, primarily a reflection of the intimate association of organic matter with mineral grains and their combined maturation history, regulate the physiochemical speciation and transport of petroleum during generation, migration, and production stages. In order to better understand the fundamental relationship between these constituents and pore network characteristics, we analyzed the variation in rock matrix microstructural properties with organic and mineral composition, distribution, and maturity in core samples from the Barnett, Woodford, Caney, Haynesville, Fayetteville, Marcellus, Mancos, and Antrim formations located in the continental United States.

Samples were petrographically described (including vitrinite reflectance) by thin section optical microscopy, and measured for total elemental (C,H,N,O,S) and organic carbon (TOC) content by combustion EA, mineral composition by FTIR spectroscopy, organic matter composition by Rock-Eval pyrolysis, py-GC/MS, and matrix microstructure by gas sorption and SEM imaging. Compositional and microstructural measurements were then repeated following the sequential removal of bitumen and kerogen via solvent extraction and combustion, respectively.

Native state samples exhibit slit-like pore geometry with pore widths ranging from <2 nm to >100 nm. Samples in the oil and gas generation thermal windows contain micropores (<2 nm) (Figure 1) that largely contribute to elevated specific surface areas ( $A_s$ ). Although not clearly correlated with TOC content,  $A_s$  thus tends to increase with maturity, reflecting the creation of such micropore cavities as kerogen is converted to higher molar volume petroleum, some of which is displaced under correspondingly higher pore pressures. This behavior is

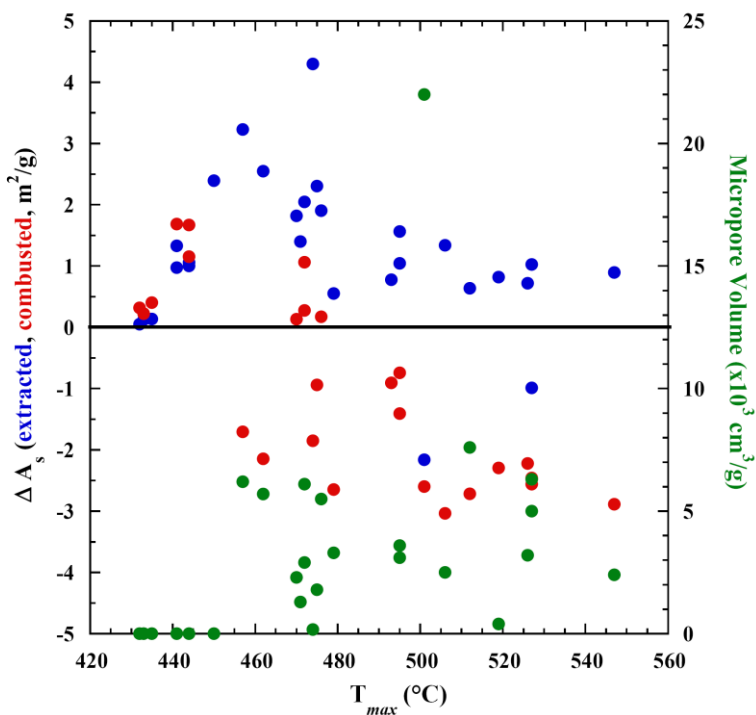


Figure 1 – Change in specific surface area of extracted and combusted shale samples relative to their native state analogues (left axis) and the volume of micropores (right axis) versus Rock-Eval  $T_{max}$ .

supported by a largely consistent rise in  $A_s$  upon bitumen extraction (Figure 1), especially during the oil generation stage, reflecting the intimate spatial association of unexpelled petroleum product with residual kerogen substrate. Subsequent removal of this kerogen through combustion results in a modest increase in  $A_s$  for less mature samples but a marked decline in their more mature counterparts (Figure 1), indicating the loss of micropore-replete mature kerogen and the attendant exposure of relatively low surface area meso- and macropore cavities. Changes in mineral composition during the combustion process may complicate this interpretation, but FTIR data indicate little modification. And although hydraulic radii of native state samples, a proxy for mean pore size, unexpectedly trend toward smaller values at higher permeabilities, combusted analogues display an opposite relationship that is more characteristic of conventional reservoirs.

In order to more directly relate the effects of thermal maturation to pore structure changes and corresponding petroleum generation, migration, and storage potential, hydrous pyrolysis experiments were performed on calcareous- and organic rich core horizons from the Barnett formation using the sealed gold capsule technique at three different time points (2, 6 and 18 days) under constant temperature (350°C) and hydrostatic pressure (250 bar) conditions. In addition to the analyses above, we monitored the composition of bitumen products by GC-MS and co-generated gas composition and isotopic signature by headspace GC and GC-IRMS.

Hydrocarbon gas yields increased over time, with the organic-rich interval generating approximately five times more  $C_1$ - $C_4$  gases (500  $\mu\text{g/g}$ ) of wetter composition ( $C_1/C_{2+} \sim 0.4$ ) after 18 days than the calcareous interval. Large amounts of  $\text{CO}_2$  (~15,000  $\mu\text{g/g}$ ), likely the result of carbonate thermal decomposition, were also generated after only 2 days and remained nearly constant thereafter. Bitumen extracts, while low in mass typical of many gas-stage shales, displayed classic early ingrowth of a broad, low CPI paraffin distribution followed by cracking to lighter compounds. Interestingly,  $A_s$  of pyrolyzed samples with and without their bitumen extracted increased initially and declined at later stages (Figure 2), possibly reflecting the initial creation and subsequent consolidation of kerogen-hosted, partially fluid-filled micropores. Coupled with FTIR and SEM data, these initial results might also hint at the importance of moisture- and heat-sensitive mineral transformations relative to their organic counterparts or the interplay of other environmental parameters such as differential fluid and interfacial chemistry. Overall, such findings highlight the importance of organic matter maturity, type, and distribution in governing the transport of both petroleum and stimulation fluids through shale matrices.

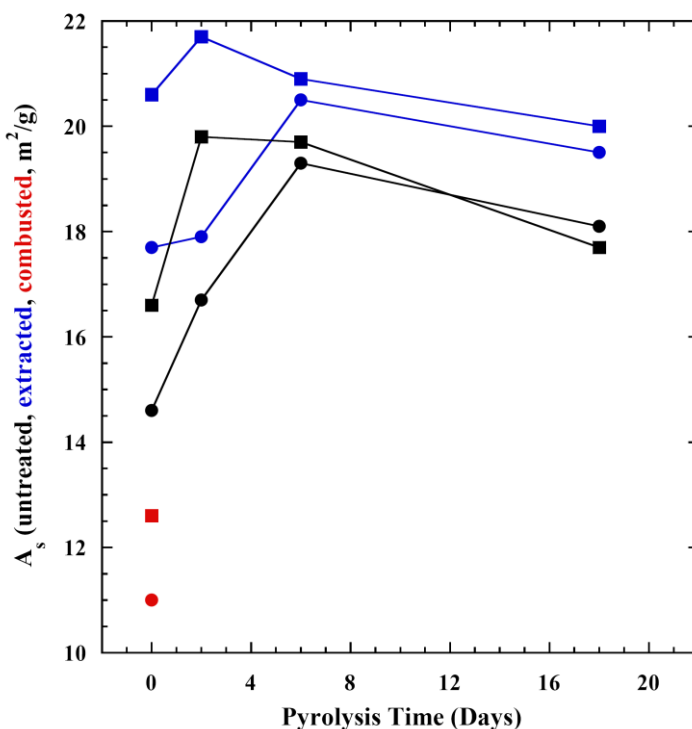


Figure 2 – Specific surface area of untreated, extracted, and combusted calcareous (circle) and OC-rich (square) shale samples as a function of artificial maturation pyrolysis time.